Journal of
Composites Science

MDPI

Communication

China Rose/*Hibiscus rosa-sinensis* Pollen-Mediated Phytosynthesis of Silver Nanoparticles and Their Catalytic Activity

Brajesh Kumar [1,2,*], Kumari Smita [1], Yolanda Angulo [1], Alexis Debut [1] and Luis Cumbal [1]

[1] Centro de Nanociencia y Nanotecnologia, Universidad de las Fuerzas Armadas ESPE, Av. Gral. Rumiñahui s/n, Sangolqui P.O. Box 171-5-231B, Ecuador
[2] Department of Chemistry, TATA College, Kolhan University, Chaibasa 833202, India
* Correspondence: krmbraj@gmail.com; Tel.: +91-875-7618-562

Abstract: We reported an ecofriendly method for the phytosynthesis of silver nanoparticles (AgNPs) using the pollen of double-petal China rose/*Hibiscus rosa-sinensis* as a natural reducing and stabilizing agent. The phytosynthesized AgNPs were preliminary characterized by their optical properties by UV–vis spectroscopy and showed their corresponding surface plasmonic resonance (SPR) at 405 nm. The distribution pattern and morphology of the synthesized AgNPs were confirmed by dynamic light scattering and transmission electron microscopy whereas X-ray diffraction and Fourier transform infrared spectroscopy depicts their surface properties and crystalline nature. The phytosynthesized AgNPs were spherical, well dispersed, 10–50 nm in size, and crystalline. It also showed moderate photocatalytic activity for the degradation (>30%, 2.5 h) of Thioflavin T dye in direct sunlight. Thus, this work highlights the importance of China rose pollen in green nanoscience and supports the cleanliness of nature by naturally available materials.

Keywords: China rose pollen; silver nanoparticles; spectroscopy; ecofriendly; photocatalysis

check for updates

Citation: Kumar, B.; Smita, K.; Angulo, Y.; Debut, A.; Cumbal, L. China Rose/*Hibiscus rosa-sinensis* Pollen-Mediated Phytosynthesis of Silver Nanoparticles and Their Catalytic Activity. *J. Compos. Sci.* **2022**, *6*, 322. https://doi.org/10.3390/jcs6110322

Academic Editor: Goshtasp Cheraghian

Received: 28 August 2022
Accepted: 17 October 2022
Published: 26 October 2022

Publisher's Note: MDPI stays neutral with regard to jurisdictional claims in published maps and institutional affiliations.

Copyright: © 2022 by the authors. Licensee MDPI, Basel, Switzerland. This article is an open access article distributed under the terms and conditions of the Creative Commons Attribution (CC BY) license (https://creativecommons.org/licenses/by/4.0/).

1. Introduction

Nowadays, the scope of nanomaterials in multifarious biomedical fields and for environmental remediation is rising, with the increasing populations, and has an impact on society. The synthesis and applications of silver-based nanostructures, that are usually in the range of 1–100 nm, are of great interest due to their unique physicochemical properties and versatile applications in catalysis [1], photocatalysis [2], antioxidants [1,2], biomedicine [3], cosmetics [4], sensing [5], drug delivery [6], food packaging [7], bio-imaging [8], solar cells [9], etc. Until now, numerous "top-down" and "bottom-up" methods for the synthesis of silver nanoparticles (AgNPs) have been reported, such as laser ablation, chemical vapor deposition, chemical reduction, microemulsion, microwave-assisted methods [10], ultrasonic-assisted methods [11], solvothermal techniques [12], sol-gel processes [13], electrochemical methods [14], and Tollens' reagents [15]. However, the majority of these methods are expensive, hazardous, and problematic for the environment.

Consequently, developing the green synthesis of AgNPs using plants, bac teria, algae, and fungi is preferred to chemical synthesis. An important point in the pro duction of nanoparticles is the use of cost-effective and efficient precursors. Interestingly, plant-derived AgNP synthesis methods are cheap, do not need special conditions, are easy to scale, safe, ecofriendly, and have played an important role in various biotechnology applications. Phytochemical compounds found in plants replace chemical reagents and improve the single route protocol as a reducing and capping agent [16]. Several studies have documented the synthesis of AgNPs using plant materials, especially flowers including *Rosa santana* [17], *Calotropis procera* [18], *Mangifera indica* [19], *Fritillaria* [20], *Lantana camara* [2], *Aerva lanata* [3], *Nyctanthes arbortristis* [21], *Bauhinia purpurea* [22], *Zephyranthes candida* [23], *Hibiscus rosa-sinensis* [24], etc., used for various biotechnology applications.

The *Hibiscus rosa-sinensis* is a small tree or shrub with evergreen flowers whose color may vary from pink, red, yellow, to orange, shown in Scheme 1. It is commonly known as the China rose, belonging to the family malvaceae, native to tropical regions of Asia, and is widely used as an ornamental species [25]. Its petals, leaves, and pollens contain sugars, polyphenols, flavonoids, amino acids, vitamins, enzymes, carotenoids, anthocyanins, citric acid, and tartaric acids [24,26]. Traditionally, the plant has many medicinal uses for treating fevers and coughs, diabetes, wound healing, bacterial and fungal infections, and gastric ulcers [27]. Nayak et al. in 2015, Periasamy et al. in 2022, and Kainat et al. in 2021reported the synthesis of AgNPs, cobalt oxide, and magnesium oxide nanoparticles using flowers, leaves, and the bark of *H. rosa sinensis* and evaluated their antimicrobial activity against different microbes [24,26,27]. As a result, *H. rosa sinensis* has attracted attention throughout the world.

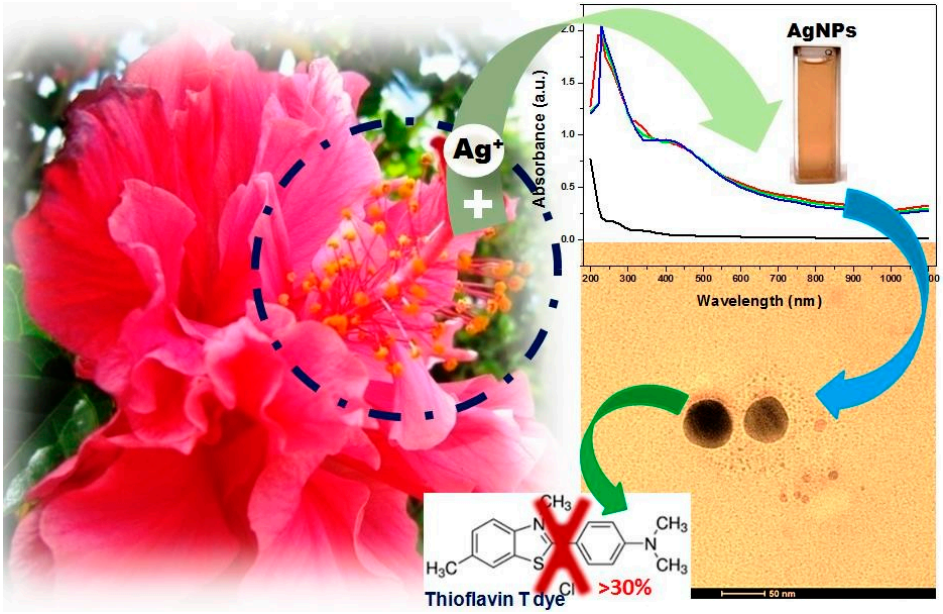

Scheme 1. Representation of *H. rosa-sinensis* pollen-assisted synthesis and characterization of AgNPs.

Until now, various types of pollen have been used to synthesize metal nanoparticles and assess their catalytic, antioxidant, and other biomedical activity. We also reported the reducing capability and antioxidant activity of bee pollen and its synthesized AgNPs [28]. However, there are no reports on the phytosynthesis of AgNPs using *H. rosa- sinensis* pollen and their photocatalytic action against dye degradation. Therefore, the main aim of this work was to synthesize AgNPs using Ag+ ion and *H. rosa-sinensis* pollen via ecofriendly routes. Furthermore, as-synthesized AgNPs have been characterized by various analytical techniques. Scheme 1 illustrates the simple, quick, selective, and ecofriendly pathway for the synthesis and characterization of AgNPs. To this end, the photocatalytic activity of AgNPs was also evaluated against the Thioflavin T (TF) dye. As we know, TF dye is a stable, sulfur-containing heterocyclic compound and has potential applications in antipyretics, photographic developers, and corrosion inhibitors. Its acute exposure can cause some harmful effects to humans [29]. Thus, the remediation of TF from wastewater using green nanomaterials is a major challenge for the scientist.

2. Experimental Section

2.1. Materials

Fresh, double-petal *H. rosa-sinensis* flowers containing pollen (Figure 1a) were collected from the residential colony, Playa Chica 1, close to the Universidad de las Fuerzas Armadas ESPE, Sangolqui, Ecuador, in the month of June 2014. All chemicals were analytical grade and used without any purification. Silver nitrate ($AgNO_3$, 99.0%) was purchased from

Spectrum, Stamford, CT, USA, and Thioflavin T (>75%) was acquired from Sigma Aldrich, St. Louis, MO, USA. Milli-Q water was used throughout the experiments.

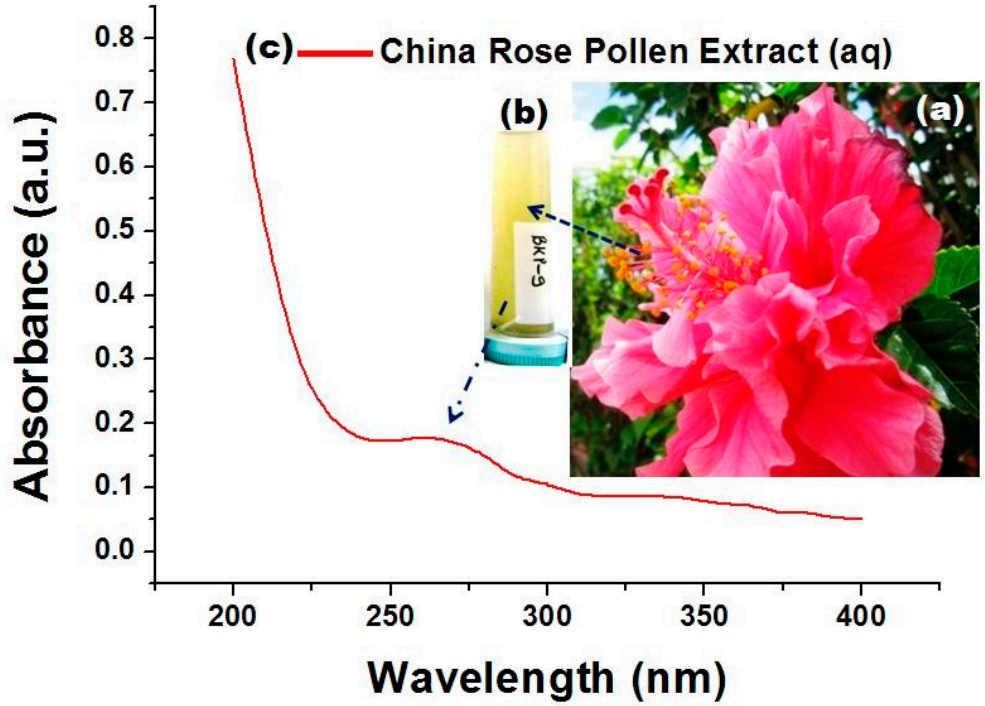

Figure 1. (**a**) Photographic image of double-petal China rose/*Hibiscus rosa-sinensis* flower, (**b**) its pollen extract, and (**c**) UV–vis spectrum of its pollen extract.

2.2. Phytosynthesis of AgNPs Using China Rose/H. rosa-sinensis Pollen

For the biosynthesis of AgNPs, 10 mg of yellow pollen grains were separated from the double-petal *H. rosa- sinensis*/China rose (Figure 1a) and added directly to a round-bottom flask containing 20 mL of 1 mM $AgNO_3$ solution, followed by stirring for 2 h at 65–67 °C. Thereafter, the color of the reaction mixture gradually changed over 30 min, and the observed brownish-yellow-color reaction mixture was incubated for the next 24 h at ambient temperature (25 ± 2 °C). The reaction mixtures were centrifuged at 5000 rpm for 4 min, to remove the pollen, and a brownish-yellow-color supernatant was obtained as AgNPs. Subsequently, the synthesized AgNPs were kept at 4 °C for the further spectroscopic and microscopic analysis.

2.3. Photocatalytic Test of AgNPs

To understand the photocatalytic properties of AgNPs, the degradation of the TF dye was studied in direct sunlight and the method was adapted by Kumar et al. in 2021 [29]. In brief, 500 µL of AgNPs and 500 µL of H_2O were added to 5 mL TF (10 mg/L). TF dye without AgNPs was used as a control. Both sets were vortexed for 5 min and then kept in the dark for the next 25 min to establish the adsorption–desorption equilibrium. Thereafter, transparent glass tubes containing a reaction mixture were kept in direct sunlight (1147–1329 cd/m^2). The progress of the degradation reaction was monitored by measuring the UV–Vis absorption spectrum between 250 and 550 nm (λ_{max} 413 nm) at different time intervals. The catalytic efficiency of the AgNPs was quantified by calculating the photocatalytic degradation percentage (%) of TF using Equation (1):

$$\eta = (A_0 - A_t)/A_0 \times 100\% \quad (1)$$

where η is the rate of degradation of TF in terms of %, A_0 is the initial absorbance of the dye solution, and At is the absorbance of the TF at time t, respectively [2,29].

2.4. Characterization of AgNPs

A digital light microscopic image of *H. rosa-sinensis* pollen was taken on a Trinocular Stereomicroscope, (SMZ745T, Nikon, Tokyo, Japan). The optical properties of AgNPs and chemical constituents of *H. rosa-sinensis* pollen were analyzed on a single-beam UV–vis spectrophotometer (Thermo Spectronic, GENESYSTM 8, England, quartz cell, path length 10 mm) using milli-Q water as a reference. The mean particle diameter of the AgNPs was measured with HORIBA, dynamic light scattering (DLS) version LB-550 program. The morpho logical and selective area electron diffraction (SAED) pattern of AgNPs was digitally recorded by transmission electron microscopy, TEM (FEI, TECNAI, G2 spirit twin, Holland) operated at an accelerated voltage of 80 kV. X-ray diffraction (XRD) analyses were performed with a PANalytical brand, θ-2θ configuration (generator–detector) X-ray tube, copper λ = 1.54059 Å, and an EMPYREAN diffractometer. The Fourier transform infrared spectroscopy (FTIR) measurement in the attenuated total reflectance (ATR) mode was conducted on the Frontier FT-IR spectrophotometer (Perkin Elmer, Waltham, MA, USA).

3. Results and Discussion

3.1. Visual and UV–Vis Studies of H. rosa-sinensis Pollen

China rose/*H. rosa-sinensis* is found almost everywhere in the world and the pollen from the pink, double-petal China rose (Figure 1a) is the subject of our study. Figure 1b,c shows the visual image and UV–vis spectrum of the aqueous extract of *H. rosa-sinensis* pollen. The aqueous extract obtained by pollen dispersal in the water was light yellow, suggesting the presence of bioactive compounds in the aqueous medium, and directly linked to plant pigments (Figure 1b). The absorption band appeared between 230 and 320 nm due to the presence of $\pi_{\rightarrow}\pi^*$ and $n_{\rightarrow}\pi^*$ electronic excitation of C=C, C=N, C=O present in sugars, polyphenolics, flavonoids, amino acids, vitamins, carotenoids, anthocyanins, and citric acid (Figure 1c) [24,26,27,30].

3.2. Microscopic and XRD Studies of H. rosa-sinensis Pollen

The light microscope image clearly visualizes that *H. rosa-sinensis* pollens are almost the same size and certain pollens are clustered (Figure 2a). All pollens appear to be spherical, rough, with a size ranging from 35 to 40 µm, and a surface covered with round-tipped spines. Similar results were reported by Andrade et al. [25]. The X-ray diffraction pattern of *H. rosa-sinensis* pollens is illustrated in Figure 2b. In most of the reports, the broad peak at the (2θ) value between 15 and 35° was attributed to the organic framework structure of the various phytochemicals/cellulose as the prime component [30]. It does not show a peak corresponding to the metal, confirming the lack of metal contamination and the amorphous/non-crystalline nature of the organic pollen molecules. Darweesh et al. in 2022 and Atalay et al. in 2020 observed the same XRD result for banana leaf powder and *Juglans* pollen without the treatment of metals [30,31].

3.3. Visual and UV–Vis Studies of AgNPs Synthesized by H. rosa-sinensis Pollen

The UV–Visible spectroscopy is one of the most common and straightforward techniques for identifying the size, shape, and distribution of nanoparticles. During the synthesis of AgNPs, the reaction mixture will undergo a set of color changes, which indicate the progress of a reaction [2,32]. Color changes are achieved due to the effect of the surface plasmon resonance (SPR) of the nanoparticles that depend on their size and shape [3]. In Figure 3a–c, the color changes from colorless to brownish yellow when *H. rosa-sinensis* pollen extract is added to the $AgNO_3$ solution and it preliminarily confirms the formation of AgNPs in the reaction mixture [33]. The successful formation of AgNPs is identified by UV–visible spectra analysis, as illustrated in Figure 3d. There is a decrease in the absorption band between 280 and 350 nm, and a new broad SPR band at approximately λ_{max} 405 nm was observed. The bioactive molecules/metabolites present in the *H. rosa-sinensis* pollen extract probably bind to Ag+, cause visual color change, and promote the formation of AgNPs by reducing Ag+ to Ag0 [28,33]. The 15-day reaction mixture shifted the SPR band

to 420 nm, confirming the formation of larger AgNPs. No change in the SPR peak position and intensity was observed for 7 days under laboratory conditions, confirming the stability of as-synthesized AgNPs without sedimentation. The stability of AgNPs may be due to the capping effect of bioactive molecules adsorbed on the surface of the synthesized nanoparticles. Similar values of λ_{max} = 405−410 nm of AgNPs synthesized from aqueous extracts of *Calotropis procera* flower [18] and *Capparis petiolaris* fruit [32] have previously been reported, corresponding to particle size within the range of 10 to 40 nm.

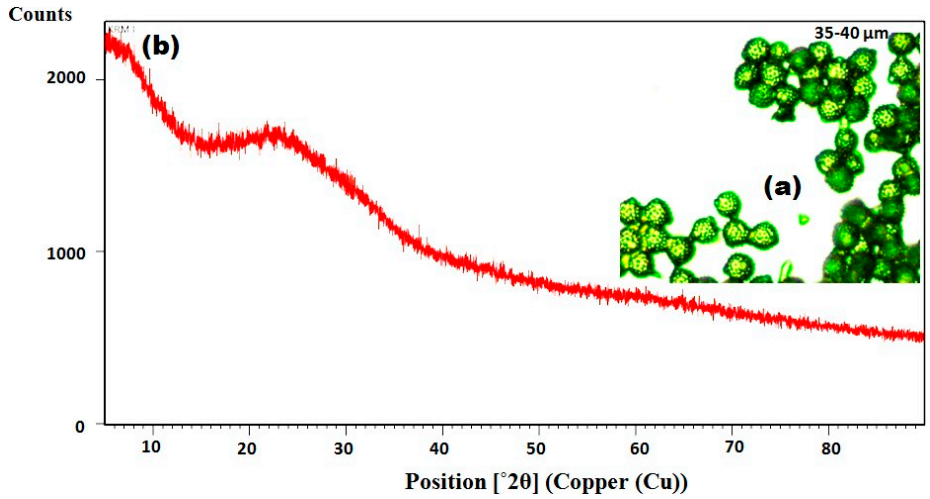

Figure 2. (**a**) Microscopic image and (**b**) XRD pattern of double-petal *H. rosa-sinensis* pollen.

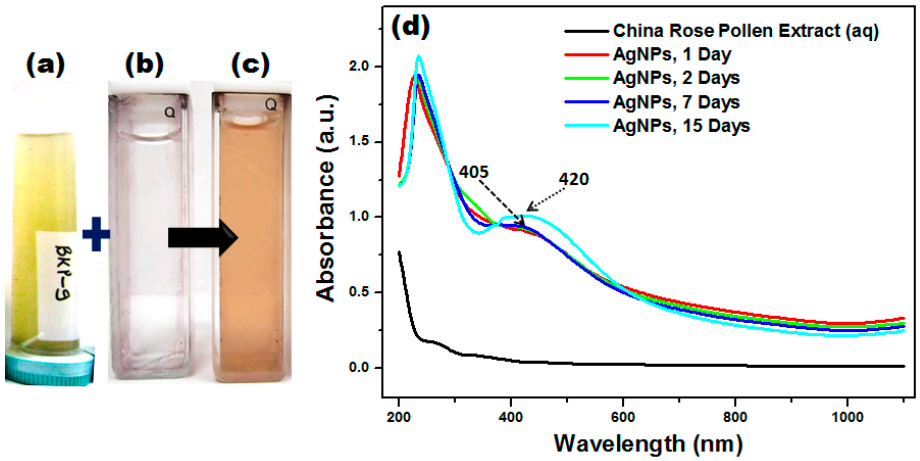

Figure 3. Visual image of (**a**) *Hibiscus rosa-sinensis* pollen extract, (**b**) 1 mM $AgNO_3$, (**c**) as-synthesized AgNPs, and (**d**) UV–vis spectrum of as-synthesized AgNPs using *Hibiscus rosa-sinensis* flower pollen at different incubation times.

3.4. DLS Studies of AgNPs

Dynamic light scattering analysis is a common tool for determining the hydrodynamic size distribution and particle size of biosynthesized AgNPs. The DLS data were plotted in Figure 4 after one day of AgNP incubation and clearly stated that the suspen sion contains different-sized nanoparticles. It explained that the average size diameter of the AgNPs was 70.4 ± 35.56 nm and its polydispersity index (PDI) was 0.2557. A PDI value greater than 0.1 refers to a broad distribution that leads to particle aggregation, the screening of smaller particles by bigger ones, organic coating on the particles, etc. [5,11,28] We reviewed the DLS and optical properties of the AgNPs stored for a month and found them to be quite satisfactory (data not shown).

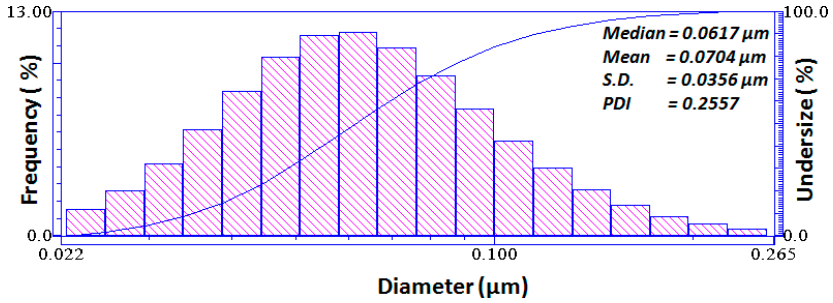

Figure 4. DLS pattern of as-synthesized AgNPs.

3.5. TEM–SAED Studies of AgNPs

The shape of particles and the average diameter were determined from the micrographs by TEM. In Figure 5a–d, TEM analysis revealed the formation of spherical and non-agglomerated AgNPs of size ranges from 10 to 50 nm. The corresponding size distribution histogram of the AgNPs seen in the TEM image (Figure 5a) was analyzed manually with the ImageJ software. It demonstrated that the mean size of the AgNPs was 25.4 ± 13.1 nm (Figure 5b). Other HR-TEM was also performed at a resolution of 50 nm and it revealed that the AgNPs were mainly spherical in shape (Figure 5c,d). A slight heating can provoke a fast reaction and favors the reduction of Ag+ ions in the formation of nuclei [16,24]. We suggest that the organic layer encapsulates the AgNPs and inhibits the agglomeration of AgNPs. The SAED analysis also provides additional supporting information (Figure 5e) and was performed from a spherical AgNPs indicated bright spots, and identifies the existence of monocrystalline elemental silver as AgNPs. The TEM result is also consistent with that of the DLS analysis. Vizuete et al. [32] indicated the formation of spherical AgNPs with a size range of 10 to 30 nm, based on UV–Visible and TEM analyses.

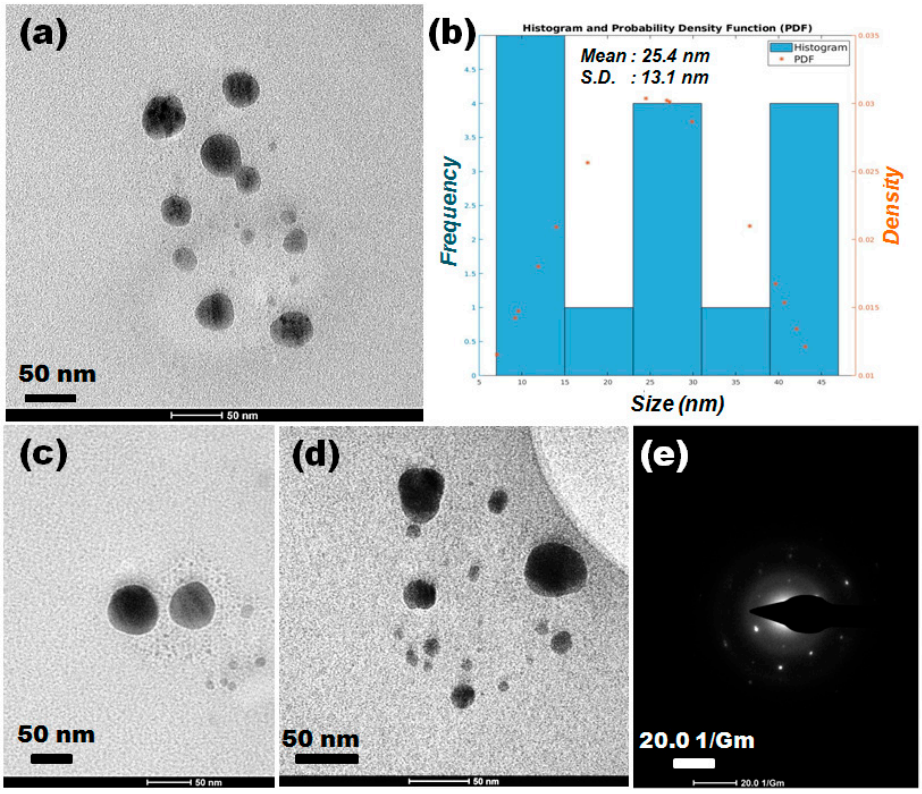

Figure 5. (**a**) TEM images of AgNPs and (**b**) its size distribution graph. Other TEM images (**c**,**d**) and (**e**) SAED pattern of as-synthesized AgNPs.

3.6. FTIR Studies of AgNPs

The FTIR spectra of AgNPs synthesized by *H. rosa-sinensis* pollen extract is shown in Figure 6. The absorption peaks at 3270 and 1016 cm^{-1} correspond to –OH/-NH stretching, and -C-O-C stretching, whilst 1638 cm^{-1} is attributed to the stretching vibration of the carbonyl group (-C=O) present in polyphenols, glycosides, amino acids, flavonoids, carotenoids, anthocyanins, and organic acids [3,5,28]. A very weak peak observed at 2800–3000 cm^{-1} and 2000–2400 cm^{-1} indicates the symmetric/asymmetric stretching frequency for H–C–H and C≡C/C≡N/C≡O+, respectively [24,30]. Thus, the presence of these characteristic bands predicts that the functional groups present in the *H. rosa-sinensis* pollen extract can facilitate the reduction of Ag+ to Ag0 and adhere to the surface of the AgNPs to promote capping and stabilization [2,32].

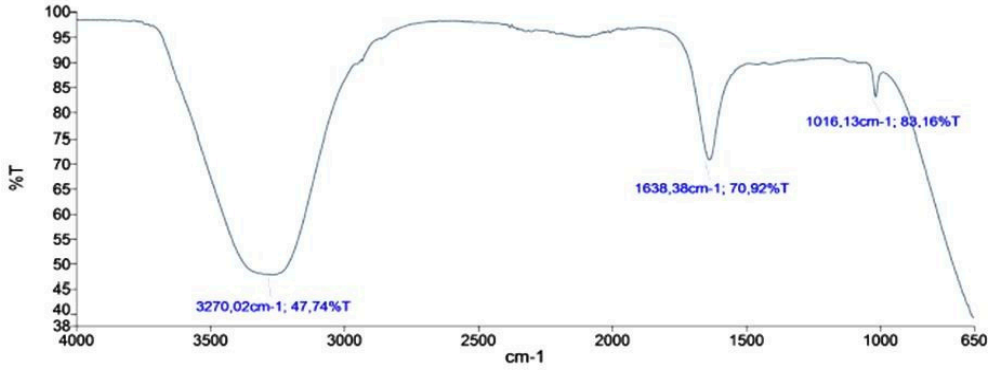

Figure 6. FTIR spectrum of as-synthesized AgNPs.

3.7. Photocatalytic Degradation Studies

The catalytic activity of various-shaped AgNPs and its nanocomposites has gained more researchers' attention due to its ecofriendliness, commercial availability, and stability [34]. Photocatalytic degradation of TF was carried out using as-synthesized AgNPs under solar light and the degradation % was estimated from the decrease in the absorption intensity of TF at characteristic λ_{max} = 413 nm at a different time [35]. In the beginning, the color of the TF dye was yellow and, after treatment with AgNPs and sunlight, the color changed to light yellow (not shown). Figure 7a indicates that the intensity of the absorption peak of TF was slightly decreased with the addition of AgNPs, which may be explained by the adsorption of TF on the surface of AgNPs [29]. However, the intensity of TF absorption gradually decreases over time, when it is directly exposed to sunlight, indicating that new compounds have formed. Complete degradation of TF was not observed; this may be due to the lack of uniformity of AgNPs, the low intensity of sunlight, or the lower potential of phytochemical-capped AgNPs [36]. In Figure 7b, the degradation % of TF by AgNPs is plotted as 8.08, 15.33, 17.66, 18.48, 25.29, 28.38, and 30.67% in 15, 30, 45, 60, 90, 120, and 150 min. The results showed that as the sunlight exposure time increases from 0 to 150 min, the % of TF degradation also increases. This is because of the presence of surface hydroxyl groups which facilitate the entrapment of photoinduced electrons and holes, thus improving the photocatalytic degradation process [37]. On the other hand, only 2.57% of TF was adsorbed on AgNPs before the photodegradation test. The degradation pattern of TF results is similar to that of previous studies, where they observed demethylation and the oxidation product of TF [29,36,37]. Therefore, green synthesized AgNPs are preferentially explored as photocatalysts instead of adsorbents.

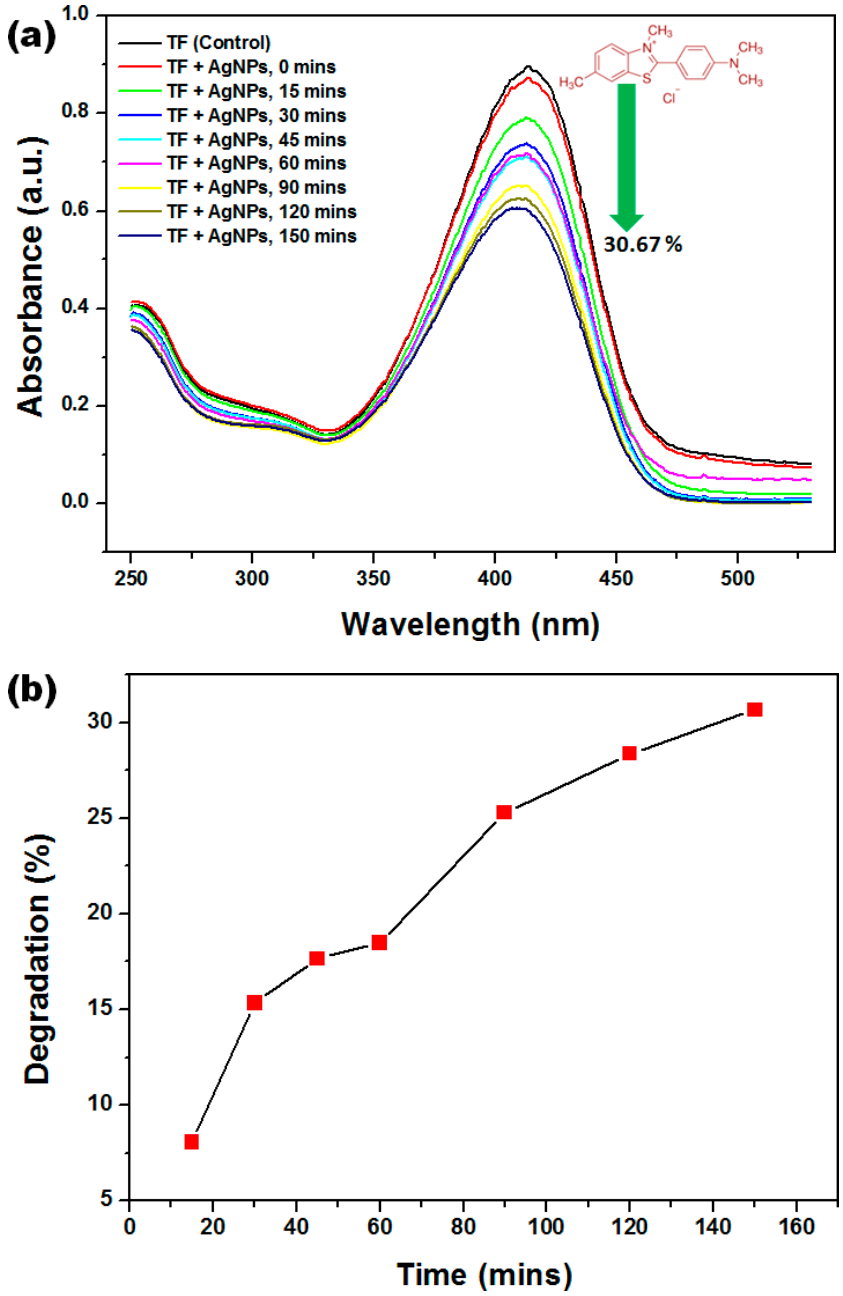

Figure 7. (**a**) Photocatalytic degradation pattern and (**b**) degradation % of TF using synthesized AgNPs at different sunlight exposure times by observing changes in absorbance at 413 nm.

4. Conclusions

It is proven that the pollen extract of *Hibiscus rosa-sinensis* acts as a reducer and stabilizer in the process of AgNP synthesis. The suggested phytochemical-based synthesis method is simple, cheap, fast, and ecologically sound. The synthesized AgNPs showed λ_{max} at 405 nm corresponding to the spherical, well-dispersed, and 10–50 nm nanoparticles. In addition, AgNPs were phytochemically coated, stable, and showed moderate photocatalytic degradation (>30%, 2.5 h) activity against TF. In the future, intensive research on pollen-assisted synthesis of other metallic nanoparticles should be conducted to foster the development of cost-effective and environmentally sustainable materials in the field of nanoscience.

Author Contributions: B.K.: Conceptualization, Data curation, Formal analysis, Writing—original draft, Writing—review & editing, Methodology, Project administration, Funding acquisition. K.S.: Conceptualization, Data curation, Formal analysis, Writing—original draft, Writing—review & editing, Methodology, Project administration. Y.A.: Formal analysis, Writing—original draft, Writing—review & editing. A.D.: Formal analysis, Writing—original draft, Writing—review & editing. L.C.: Writing—original draft, Writing—review & editing, Methodology, Project administration. All authors have read and agreed to the published version of the manuscript.

Funding: This research received funding from Universidad de las Fuerzas Armadas ESPE, Ecuador, and Prometeo Project of the National Secretariat of Higher Education, Science, Technology, and Innovation (SENESCYT), Ecuador.

Institutional Review Board Statement: Not applicable.

Informed Consent Statement: Not applicable.

Acknowledgments: This scientific work has been funded by the (a) Universidad de las Fuerzas Armadas ESPE, Ecuador, (b) Prometeo Project of the National Secretariat of Higher Education, Science, Technology, and Innovation (SENESCYT), Ecuador, and (c) TATA College, Chaibasa, India.

Conflicts of Interest: The authors declare no conflict of interest.

References

1. Abdullah, H.S.T.S.; Asseri, S.N.A.R.M.; Mohamad, W.N.K.W.; Kan, S.-Y.; Azmi, A.A.; Julius, F.S.Y.; Chia, P.W. Green synthesis, characterization and applications of silver nanoparticle mediated by the aqueous extract of red onion peel. *Environ. Pollut.* **2021**, *271*, 116295. [CrossRef]
2. Kumar, B.; Smita, K.; Cumbal, L. Biosynthesis of silver nanoparticles using *Lantana camara* flower extract and its application. *J. Sol-Gel. Sci. Technol.* **2016**, *78*, 285–292. [CrossRef]
3. Kanniah, P.; Radhamani, J.; Chelliah, P.; Muthusamy, N.; Thangapandi, E.J.J.S.B.; Thangapandi, J.R.; Balakrishnan, S.; Shanmugam, R. Green Synthesis of multifaceted silver nanoparticles using the flower extract of *Aerva lanata* and evaluation of its biological and environmental applications. *Chem. Sel.* **2020**, *5*, 2322–2331. [CrossRef]
4. Arroyo, G.V.; Madrid, A.T.; Gavilanes, A.F.; Naranjo, B.; Debut, A.; Arias, M.T.; Angulo, Y. Green synthesis of silver nanoparticles for application in cosmetics. *J. Environ. Sci. Health Part A* **2020**, *55*, 1304–1320. [CrossRef] [PubMed]
5. Kumar, B.; Smita, K.; Awasthi, S.K.; Debut, A.; Cumbal, L. *Capsicum baccatum* (Andean Chilli)-assisted phytosynthesis of silver nanoparticles and their H_2O_2 sensing ability. *Part. Sci. Technol.* **2022**, *40*, 772–780. [CrossRef]
6. Prasher, P.; Sharma, M.; Mudila, H.; Gupta, G.; Sharma, A.K.; Kumar, D.; Bakshi, H.A.; Negi, P.; Kapoor, D.N.; Chellappan, D.K.; et al. Emerging trends in clinical implications of bio-conjugated silver nanoparticles in drug delivery. *Colloid Interface Sci. Commun.* **2020**, *35*, 100244. [CrossRef]
7. Istiqola, A.; Syafiuddin, A. A review of silver nanoparticles in food packaging technologies: Regulation, methods, properties, migration, and future challenges. *J. Chin. Chem. Soc.* **2020**, *57*, 1942–1956. [CrossRef]
8. Yan, N.; Tang, B.Z.; Wang, W.-X. In Vivo bioimaging of silver nanoparticle dissolution in the gut environment of zooplankton. *ACS Nano* **2018**, *12*, 12212–12223. [CrossRef]
9. Kalfagiannis, N.; Karagiannidis, P.G.; Pitsalidis, C.; Panagiotopoulos, N.T.; Gravalidis, C.; Kassavetis, S.; Patsalas, P.; Logothetidis, S. Plasmonic silver nanoparticles for improved organic solar cells. *Sol. Energy Mater. Sol. Cells* **2012**, *104*, 165–174. [CrossRef]
10. Beyene, H.D.; Werkneh, A.A.; Bezabh, H.K.; Ambaye, T.G. Synthesis paradigm and applications of silver nanoparticles (AgNPs), A review. *Sustain. Mater. Technol.* **2017**, *13*, 18–23. [CrossRef]
11. Guzmán, K.; Kumar, B.; Vallejo, M.J.; Grijalva, M.; Debut, A.; Cumbal, L. Ultrasound-assisted synthesis and antibacterial activity of gallic acid-chitosan modified silver nanoparticles. *Prog. Org. Coat.* **2019**, *129*, 229–235. [CrossRef]
12. Mahltig, B.; Gutmann, E.; Reibold, M.; Meyer, D.; Bottcher, H. Synthesis of Ag and Ag/Si_{O2} sols by solvothermal method and their bactericidal activity. *J. Sol-Gel. Sci. Technol.* **2009**, *51*, 204–214. [CrossRef]
13. Tarimala, S.; Kothari, N.; Abidi, N.; Hequet, E.; Fralick, J.; Dai, L.L. New approach to antibacterial treatment of cotton fabric with silver nanoparticle–doped silica using sol–gel process. *J. Appl. Polym. Sci.* **2006**, *101*, 2938–2943. [CrossRef]
14. Ma, H.; Yin, B.; Wang, S.; Jiao, Y.; Pan, W.; Huang, S.; Chen, S.; Meng, F. Synthesis of silver and gold nanoparticles by a novel electrochemical method. *Chem. Phys. Chem.* **2004**, *24*, 68–75. [CrossRef]
15. Soukupova, J.; Kvitek, L.; Panacek, A.; Nevecna, T.; Zboril, R. Comprehensive study on surfactant role on silver nanoparticles (NPs) prepared via modified Tollens process. *Mater. Chem. Phys.* **2008**, *111*, 77–81. [CrossRef]
16. Aisida, S.O.; Ugwoke, E.; Uwais, A.; Iroegbu, C.; Botha, S.; Ahmad, I.; Maaza, M.; Ezema, F.I. Incubation period induced biogenic synthesis of PEG enhanced *Moringa oleifera* silver nanocapsules and its antibacterial activity. *J. Polym. Res.* **2019**, *26*, 225. [CrossRef]
17. Jahan, I.; Erci, F.; Isildak, I. Microwave-assisted green synthesis of non-cytotoxic silver nanoparticles using the aqueous extract of *Rosa santana* (rose) petals and their antimicrobial activity. *Anal. Lett.* **2019**, *52*, 1860–1873. [CrossRef]

18. Babu, S.A.; Prabu, H.G. Synthesis of AgNPs using the extract of *Calotropis procera* flower at room temperature. *Mater. Lett.* **2011**, *65*, 1675–1677. [CrossRef]
19. Ameen, F.; Srinivasan, P.; Selvankumar, T.; Kamala-Kannan, S.; Al Nadhari, S.; Almansob, A.; Dawoud, T.; Govarthanan, M. Phytosynthesis of silver nanoparticles using *Mangifera indica* flower extract as bioreductant and their broad-spectrum antibacterial activity. *Bioorg. Chem.* **2019**, *88*, 102970. [CrossRef]
20. Hemmati, S.; Rashtiani, A.; Zangeneh, M.M.; Mohammadi, P.; Zangeneh, A.; Veisi, H. Green synthesis and characterization of silver nanoparticles using *Fritillaria* flower extract and their antibacterial activity against some human pathogens. *Polyhedron* **2019**, *158*, 8–14. [CrossRef]
21. Gogoi, N.; Babu, P.J.; Mahanta, C.; Bora, U. Green synthesis and characterization of silver nanoparticles using alcoholic flower extract of *Nyctanthes arbortristis* and in vitro investigation of their antibacterial and cytotoxic activities. *Mater. Sci. Eng. C* **2015**, *46*, 463–469. [CrossRef] [PubMed]
22. Chinnappan, S.; Kandasamy, S.; Arumugam, S.; Seralathan, K.K.; Thangaswamy, S.; Muthusamy, G. Biomimetic synthesis of silver nanoparticles using flower extract of *Bauhinia purpurea* and its antibacterial activity against clinical pathogens. *Environ. Sci. Pollut. Res.* **2018**, *25*, 963–969. [CrossRef] [PubMed]
23. Kaliammal, R.; Parvathy, G.; Maheshwaran, G.; Velsankar, K.; Devi, V.K.; Krishnakumar, M.; Sudhahar, S. *Zephyranthes candida* flower extract mediated green synthesis of silver nanoparticles for biological applications. *Adv. Powder Technol.* **2021**, *32*, 4408–4419. [CrossRef]
24. Nayak, D.; Ashe, S.; Rauta, P.R.; Nayak, B. Biosynthesis, characterisation and antimicrobial activity of silver nanoparticles using *Hibiscus rosa-sinensis* petals extracts. *IET Nanobiotechnol.* **2015**, *9*, 288–293. [CrossRef] [PubMed]
25. Andrade, K.; Guerra, S.; Debut, A. Fullerene-Based Symmetry in *Hibiscus rosa*-sinensis Pollen. *PLoS ONE* **2014**, *9*, e102123. [CrossRef] [PubMed]
26. Periasamy, S.; Jegadeesan, U.; Sundaramoorthi, K.; Rajeswari, T.; Tokala, V.N.B.; Bhattacharya, S.; Muthusamy, S.; Sankoh, M.; Nellore, M.K. Comparative analysis of synthesis and characterization of silver nanoparticles extracted using leaf, flower, and bark of *Hibiscus rosa sinensis* and examine its antimicrobicidal activity. *J. Nanomater.* **2022**, *2022*, 8123854. [CrossRef]
27. Kainat; Khan, M.A.; Ali, F.; Faisal, S.; Rizwan, M.; Hussain, Z.; Zaman, N.; Afsheen, Z.; Uddin, M.N.; Bibi, N. Exploring the therapeutic potential of *Hibiscus rosa* sinensis synthesized cobalt oxide (Co_3O_4-NPs) and magnesium oxide nanoparticles (MgO-NPs). *Saudi J. Biol. Sci.* **2021**, *28*, 5157–5167. [CrossRef]
28. Kumar, B.; Smita, K.; Angulo, Y.; Debut, A.; Cumbal, L. Single-step biogenic synthesis of silver nanoparticles using honeybee-collected pollen. *Inorg. Nano-Met. Chem.* 2022, *in press*. [CrossRef]
29. Kumar, B.; Smita, K.; Debut, A.; Cumbal, L. Green synthesis of cuprous oxide nanoparticles using Andean Capuli (*Prunus serotina* Ehrh. var. Capuli) Cherry. *J. Clust. Sci.* **2021**, *32*, 1753–1760. [CrossRef]
30. Darweesh, M.A.; Elgendy, M.Y.; Ayad, M.I.; Ahmed, A.M.M.; Elsayed, N.M.K.; Hammad, W.A. A unique, inexpensive, and abundantly available adsorbent: Composite of synthesized silver nanoparticles (AgNPs) and banana leaves powder (BLP). *Heliyon* **2022**, *8*, e09279. [CrossRef]
31. Atalay, F.E.; Bingol, A.; Kaya, H.; Emre, Y.; Bas, H.H.; Culum, A.A. *Juglans* Sporopollenin for High-Performance Supercapacitor Electrode Design. *ACS Omega* **2020**, *5*, 20417–20427. [CrossRef] [PubMed]
32. Vizuete, K.S.; Guzman, K.; Kumar, B.; Debut, A.; Cumbal, L. Shora (*Capparis petiolaris*) fruit mediated green synthesis and application of silver nanoparticles. *Green Process Synth* **2017**, *6*, 23–30. [CrossRef]
33. Das, T.K.; Ganguly, S.; Remanan, S.; Das, N.C. Temperature-dependent study of catalytic Ag nanoparticles entrapped resin nanocomposite towards reduction of 4-nitrophenol. *ChemistrySelect* **2019**, *4*, 3665–3671.
34. Das, T.K.; Ganguly, S.; Remanan, S.; Ghosh, S.; Das, N.C. Mussel-inspired Ag/poly(norepinephrine)/MnO_2 heterogeneous nanocatalyst for efficient reduction of 4-nitrophenol and 4-nitroaniline: An alternative approach. *Res. Chem. Intermed.* **2020**, *46*, 3629–3650. [CrossRef]
35. Fodera, V.; Groenning, M.; Vetri, V.; Librizzi, F.; Spagnolo, S.; Cornett, C.; Olsen, L.; Van de Weert, M.; Leone, M. Thioflavin T hydroxylation at basic ph and its effect on amyloid fibril detection. *J. Phys. Chem. B* **2008**, *112*, 15174–15181. [CrossRef]
36. Al-Maqdi, K.A.; Hisaindee, S.M.; Rauf, M.A.; Ashraf, S.S. Comparative degradation of a thiazole pollutant by an advanced oxidation process and an enzymatic approach. *Biomolecules* **2017**, *7*, 64. [CrossRef]
37. Kumar, B. Green Synthesis of Gold, Silver, and Iron nanoparticles for the degradation of organic pollutants in wastewater. *J. Compos. Sci.* **2021**, *5*, 219. [CrossRef]